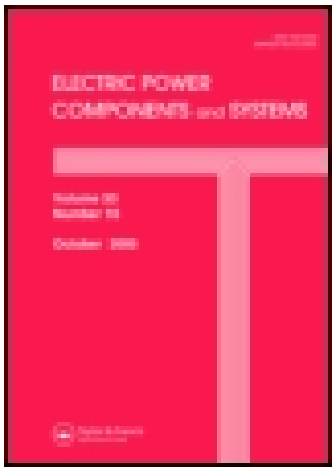

Electric Power Components and Systems
Publication details, including instructions for authors and subscription information:
http://www.tandfonline.com/loi/uemp20

Spectral Analysis for Current and Temperature Measurements in Power Cables

Sezai Taskin [a] , Serhat Seker [b] , Murat Karahan [c] & Tahir Cetin Akinci [d]
[a] Industrial Automation Department , Celal Bayar University , Manisa, Turkey
[b] Electrical Engineering Department , Istanbul Technical University , Istanbul, Turkey
[c] Electronics and Computer Education Department , Dumlupinar University , Kutahya, Turkey
[d] Electrical Education Department , Kirklareli University , Kirklareli, Turkey
Published online: 19 Mar 2009.

To cite this article: Sezai Taskin , Serhat Seker , Murat Karahan & Tahir Cetin Akinci (2009) Spectral Analysis for Current and Temperature Measurements in Power Cables, Electric Power Components and Systems, 37:4, 415-426, DOI: 10.1080/15325000802548889

To link to this article: http://dx.doi.org/10.1080/15325000802548889

Electric Power Components and Systems, 37:415–426, 2009

ISSN: 1532-5008 print/1532-5016 online
DOI: 10.1080/15325000802548889

Taylor & Francis
Taylor & Francis Group

Spectral Analysis for Current and Temperature Measurements in Power Cables

SEZAI TASKIN,[1] SERHAT SEKER,[2] MURAT KARAHAN,[3] and TAHIR CETIN AKINCI[4]

[1]Industrial Automation Department, Celal Bayar University, Manisa, Turkey
[2]Electrical Engineering Department, Istanbul Technical University, Istanbul, Turkey
[3]Electronics and Computer Education Department, Dumlupınar University, Kutahya, Turkey
[4]Electrical Education Department, Kirklareli University, Kirklareli, Turkey

Abstract *This research aims to detect spectral properties under thermal and current variations for power cables. Therefore, spectral diversities are exposed under current unbalances and different load conditions through the spectral analysis techniques. Also, huge load variations are easily detected from the current signals in the time-frequency plane using the short-time frequency analysis. Hence, this study presents the determination of the frequency characteristics and spectral similarities between the phase currents and thermal variations.*

Keywords power cables, spectral analysis, coherence, current, thermal variation

1. Introduction

In Turkey, electric power is usually transmitted by overhead lines. Power cables are less sensitive to weather and environmental conditions and, therefore, more reliable than overhead lines. Also, power cables have less influence on the environment and are less space consuming [1].

Recently, in urban areas, due to safety and aesthetic considerations, electrical energy distribution is made using underground power cables. It is important to calculate the cable lifetime. The lifetime of the cables generally depend on the cable temperature. It depends on the current passing through the cable conductor, cable structure, properties of the cable material, thermal properties of the soil around the cable, ambient temperature, and moisture content of the surrounding soil. In addition to the $I^2.R$ losses in the conductor, there are also losses in the sheath and armor of cables due to circulating currents. In some cases, eddy currents may be of consequence. The alternating voltage over the insulation also gives rise to dielectric losses, which become thermally significant in extra high-voltage cables [2].

Received 23 January 2008; accepted 15 September 2008.
Address correspondence to Dr. Sezai Taskin, Industrial Automation Department, Turgutlu Vocational College, Celal Bayar University, Turgutlu-Manisa, 45400, Turkey. E-mail: sezai.taskin@bayar.edu.tr

Nomenclature

$x(t)$	a signal
$g(t)$	a fixed-dimension window
τ	centered time location
Δf	frequency resolution
Δt	data sampling interval
γ_{xy}	coherence function
S_{xx}, S_{yy}	APSD of $x(t)$ and $y(t)$
S_{xy}	CPSD between $x(t)$ and $y(t)$

Abbreviations

STFT	short-time Fourier transform
APSD	auto-power spectral density
CPSD	cross-power spectral density

There are two heat sources in a power cable. The first heat source is generated in the conductor due to resistive losses caused by the load current, while the second is generated in the insulation due to dielectric (resistive and polarization) losses. Some of the revealed heat is absorbed by the cable, and the rest is dissipated to the surrounding soil. If the rate of heating inside the cable exceeds the rate of heat dissipation to the surroundings, the temperature of the insulation increases, and then this situation increases a risk of thermal breakdown [1]. In order to investigate this situation of risk, some analytical and numerical methods have been recently proposed in power cable literature [3–5].

Thermal ratings are critically important for cables, particularly transmission cables, since they often limit overall circuit capacity. The location along the cable route with the highest temperature will limit the overall circuit capacity, and in extreme cases, it causes thermal failure [6].

Losses, heating, and ampacity are unavoidable parameters in underground cable design, depending on cable materials, laying condition of the cable system, thermal properties of the media, bonding arrangement, etc. The electric-thermal model is outlined in a few steps: (1) loss evaluation; (2) heating evaluation; (3) electric-thermal coupling; and (4) ampacity evaluation [7].

In the related literature, there are many studies over the thermal behavior of the power cables. While part of these studies is related to the methods that are recommended according to the IEC 287 standards, another part is connected with the applications of various numerical methods. The most important first study that was based on the heat transfer calculations in the power cables is given by Whitehead and Hutchings in 1938 [8]. Another important study was that of Neher and McGrath in 1957 [9], and many other studies with this subject matter have been seen in the literature. Meanwhile, the first book based on the IEEE articles was published by Anders [10], and this book was accepted as a reference book that is related to the calculation of the maximum current carrying value without excessive heating [11]. The second book of Anders, which contains the calculations about the power cables established in some unsuitable conditions, was published in 2005 [12].

Although there are many studies based on the numerical methods in literature, real-time applications have been considered in the last 30 years, and real-time rating systems for power cables have been a commercial concern for 20 years in the world. A decent review of the past art was provided in [13].

In this study, a different approach is considered as an alternative tool to numerical methods presented in the literature. In addition, evaluating both the current and thermal variations in power cables is realized by using spectral methods such as the coherence

approach. As a result, under the current imbalances and excessive load conditions, electrical and thermal features of the power cable are extracted in the frequency domain. Hence, the signal processing application is easily adapted to monitor studies in power cables.

2. Mathematical Methods

2.1. STFT and Other Spectral Analysis Methods

The STFT, introduced by Gabor in 1946, is useful in presenting the time localization of frequency components of signals. The STFT spectrum is obtained by windowing the signal through a fixed-dimension window. The signal may be considered to be approximately stationary in this window. The window dimension fixes both time and frequency resolutions. To define the STFT, let us consider a signal $x(t)$ with the assumption that it is stationary when it is windowed through a fixed-dimension window $g(t)$, centered at time location τ. The Fourier transform of the windowed signal yields the STFT [14]:

$$STFT(\tau, f) = \int_{-\infty}^{+\infty} x(t)g(t-\tau)\exp[-j2\pi ft]\,dt. \tag{1}$$

This equation maps the signal into a two-dimensional function in the time-frequency (t, f)-plane. The analysis depends on the chosen window $g(t)$. Once the window $g(t)$ is chosen, the STFT resolution is fixed over the entire time-frequency plane.

A common approach for extracting the information about the frequency features of a random signal is to transform the signal to the frequency domain by computing the discrete Fourier transform. For a block of data of length N samples, the transform at frequency $m\Delta f$ is given by

$$X(m\Delta f) = \sum_{k=0}^{N-1} x(k\Delta t)\exp[-j2\pi km/N], \tag{2}$$

where Δf is the frequency resolution, and Δt is the data-sampling interval. The APSD of $x(t)$ is estimated as

$$S_{xx}(f) = \frac{1}{N}|X(m\Delta f)|^2, \qquad f = m\Delta f. \tag{3}$$

The CPSD between $x(t)$ and $y(t)$ is similarly estimated. The statistical accuracy of the estimate in Eq. (2) increases as the number of data points or the number of blocks of data increases.

The cause and effect relationship between two signals or the commonality between them is generally estimated using the coherence function. The coherence function is given by

$$\gamma_{xy}(f) = \frac{|S_{xy}(f)|}{\sqrt{S_{xx}(f)S_{yy}(f)}}, \qquad 0 < \gamma_{xy} < 1, \tag{4}$$

where S_{xx} and S_{yy} are the APSDs of $x(t)$ and $y(t)$, respectively, and S_{xy} is the CPSD between $x(t)$ and $y(t)$. A value of coherence close to unity indicates a highly linear and close relationship between the two signals [15, 16].

Table 1
Radius values of the power cable

Components of the cable	Radius (mm)
Phase conductor (r_1)	4.3
Neutral conductor (r_2)	3.4
Sheath material (r_3)	13.4
Outer sheath (r_4)	18.2

3. Experimental Study and Data Collection

3.1. Power Cable Specifications

Experimental data was recorded using a low-voltage underground power cable that belonged to a transformer factory. The installed power capacity of the foundation is 250 kVA. The power cable was insulated with PVC, and its voltage level is 0.6/1 kV. Specifications of the cable are given in Table 1, and schematic representation is shown in Figure 1.

In Figure 1, O is center of the cable; O_1 and O_2 represent phase and neutral conductor centers, respectively. Thickness of insulator (d_{S1}) for each phase conductor is 0.54 mm, and neutral conductor insulator (d_{S2}) is also 0.33 mm.

3.2. Recording Temperature and Current Data

In order to measure the temperature variations on the surface of the power cable, National Instruments (NI) LabVIEW 7.1 program (National Instruments™, USA) and NI FieldPoint thermocouple module, FP-TC-120 (National Instruments™, USA), were used. Experiment setup is shown in Figure 2, and Figure 3 shows the LabVIEW visual front panel. Here, LabVIEW is a graphically based programming language developed by NI [17].

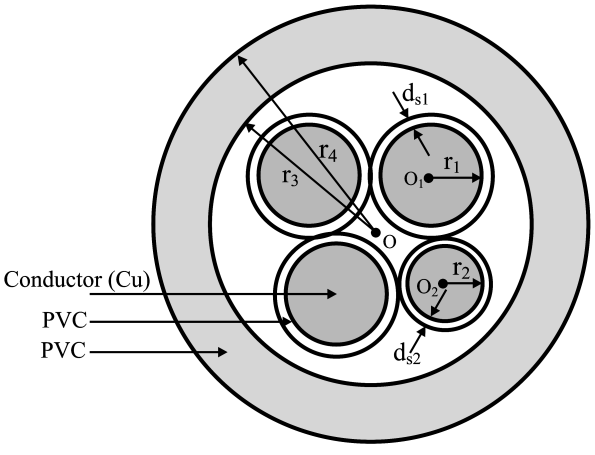

Figure 1. The power cable cross-section.

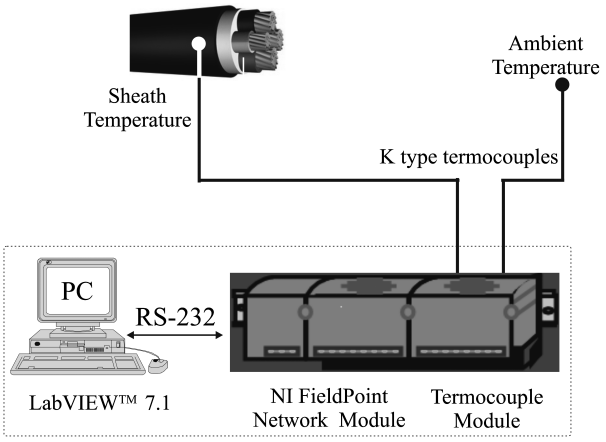

Figure 2. Experiment set-up and system configuration.

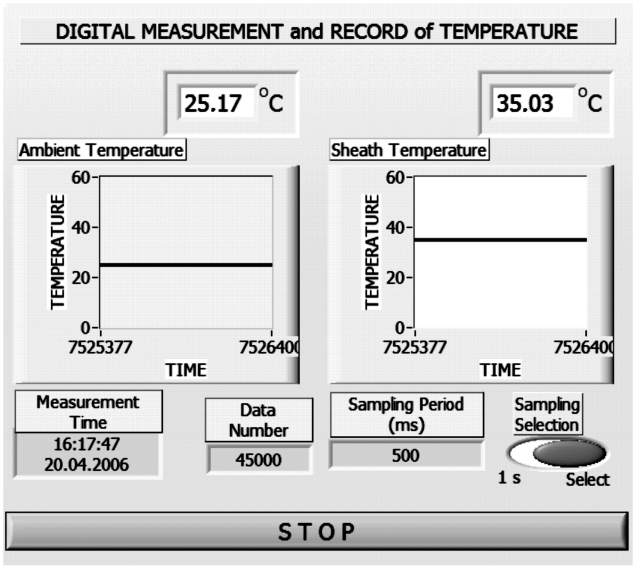

Figure 3. Temperature analysis graphic user interface, LabVIEW front panel.

Also, currents and voltage variations were measured using a power analyzer. These data were recorded simultaneously with the temperature fluctuations revealed in the power cable. Time intervals in data recording are 10, 30, and 60 sec.

4. Application to Data and Results

4.1. Spectral Calculations for Collected Data

Current variations for each phase of the cables are between the 50 A and 250 A, in addition to this, cable surface temperature also fluctuates around 30°C–55°C. All

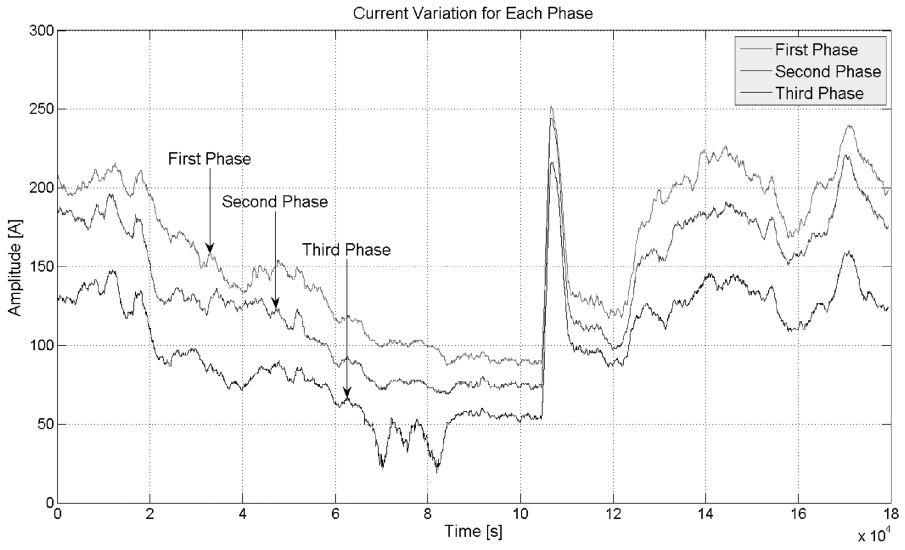

Figure 4. Current time series for each phase.

measurements are taken from the power cable in the room; the power cable that comes from the underground is, during the measurement, out of the soil. For this reason, the most important effect is related to the current load, because during the operating time of 24 hr, all working components like block heaters, ventilation motors, vacuum pumps, and compressors, have switch on or off positions. These operational diversities cause important load changes. Figure 4 shows this current variation during the two days, and Figure 5 shows temperature variation.

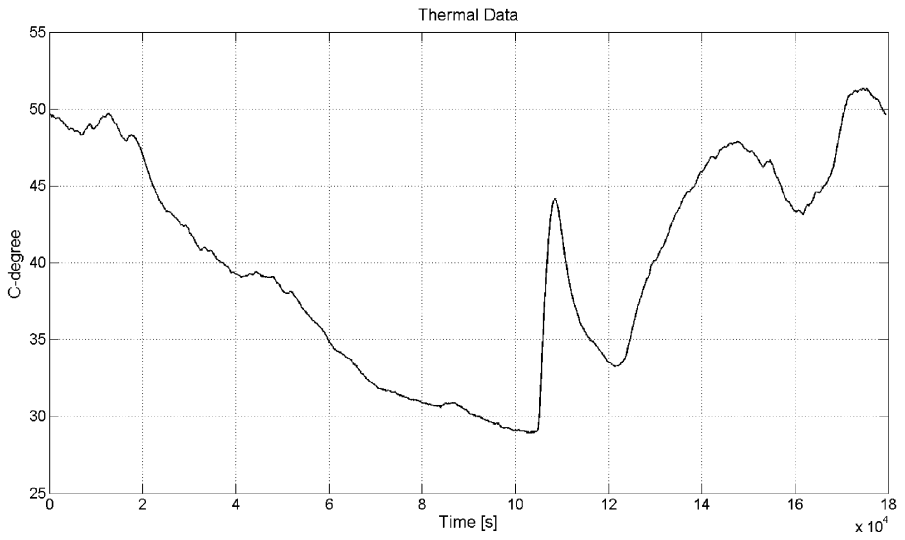

Figure 5. Temperature variation.

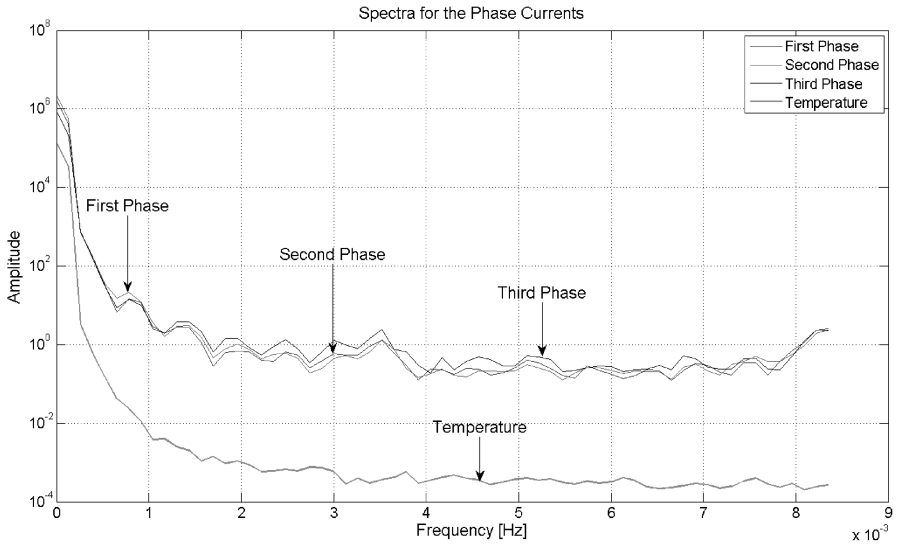

Figure 6. Spectra for the phase currents and temperature.

As seen in Figures 4 and 5, a huge peak at around 11×10^4 sec is observed; this peak value is connected with the incipient load changes based on the block heaters. Also, current variation of the third phase reflects the different characteristics from the others. This situation is related to the different load characteristics, which are fed by the third phase. If the power spectral density function for each phase current and the thermal variation data are calculated, the results are as shown in Figure 6 for the spectral variation of these quantities represented in the frequency domain. According to this figure, separation among the three phases is more apparent between the 1.5×10^{-3} Hz and 5.5×10^{-3} Hz in terms of the third phase.

Figures 7, 8, 9, and 10 show the time-frequency representation of the three phase currents and temperature variation, respectively. According to these figures, the effect of the huge peak value is easily observed around the 11×10^4 sec and 0.4×10^{-3} Hz. This localization reflects the power of the STFT. Hence, incipient load changes can be determined in the time-frequency plane. These are presented as a common result of this research.

In Figure 9, a certain band within the 0.4–7 $\times 10^{-3}$ Hz, which occurs between 6.5×10^4 sec and 8×10^4 sec of the time axis, represents fluctuation related to the third phase current, as shown in Figure 4. The harmonic frequency effect (approximately the 20th harmonic) appeared around the 11×10^4 sec is also indicated in the related figures for each phase.

4.2. Coherence Analysis

After the calculation of power spectral density functions for current and thermal data, it was determined that the thermal data variation follows the current spectra, as seen in Figure 6. However, to show the difference among the three phase currents, the coherence analysis approach is used as an alternative method. Therefore, the compar-

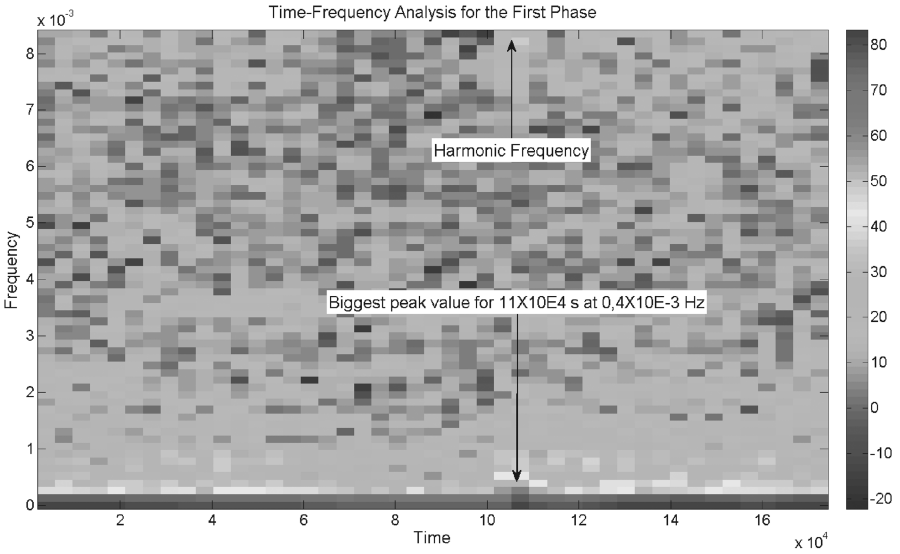

Figure 7. Time-frequency analysis for the first phase.

ison can be given through the coherence variation of the phase currents by Figure 11. Figure 11 reflects the similarity degree among the phase currents in the frequency domain. If a short-frequency region for the coherence variations (presented in Figure 11) can be considered between $0–4 \times 10^{-4}$ Hz, then the coherence variations become clearer for the low-frequency region of this comparison. This situation can be shown by Figure 12.

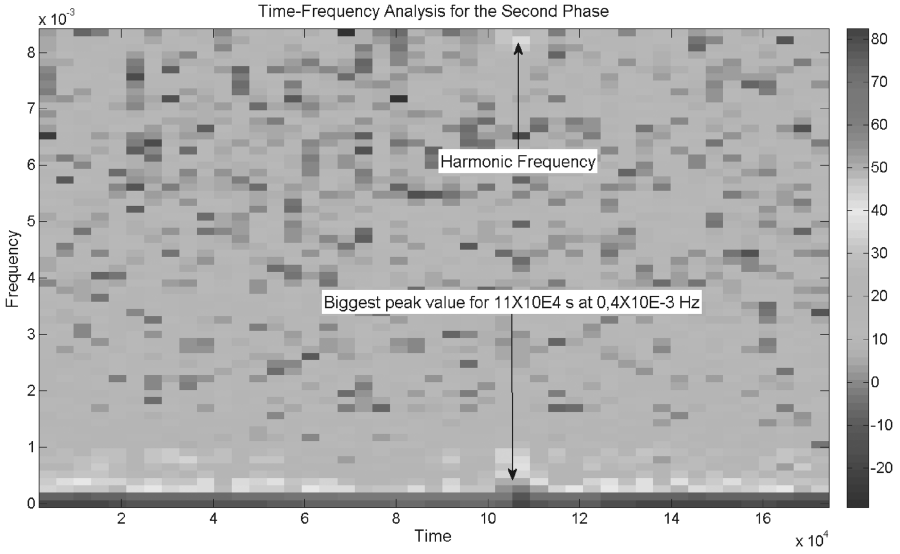

Figure 8. Time-frequency analysis for the second phase.

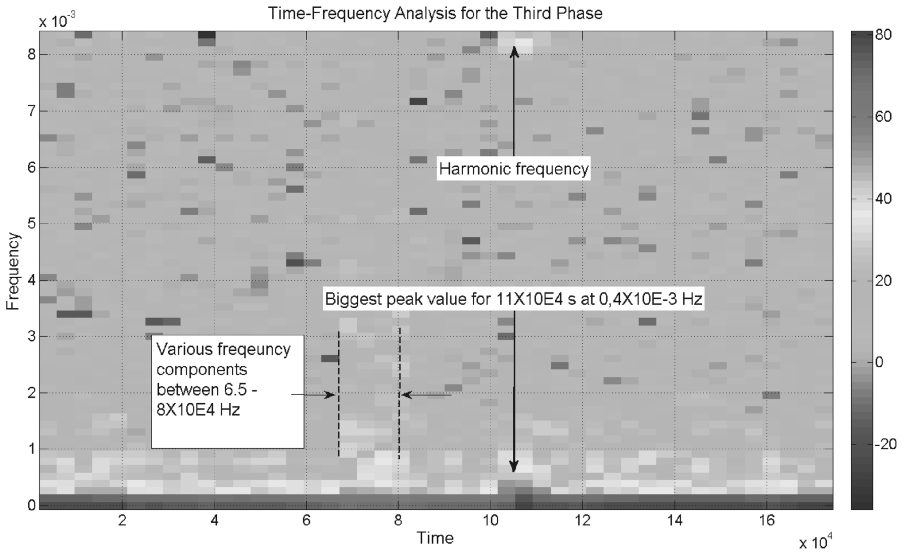

Figure 9. Time-frequency analysis for the third phase.

As seen in Figure 12, for up to 1.3×10^{-4} Hz, all phase currents are correlated with each other; however, as indicated in the short-time Fourier analysis, the most important peak value of the currents and thermal variation are localized at around 0.4×10^{-3} Hz and 11×10^4 sec for 44°C, as indicated in Figures 7–10. These characteristic values play an important role to show the distinction among the phase currents using their coherence variation according to thermal data. Hence, while Figure 11 shows the high

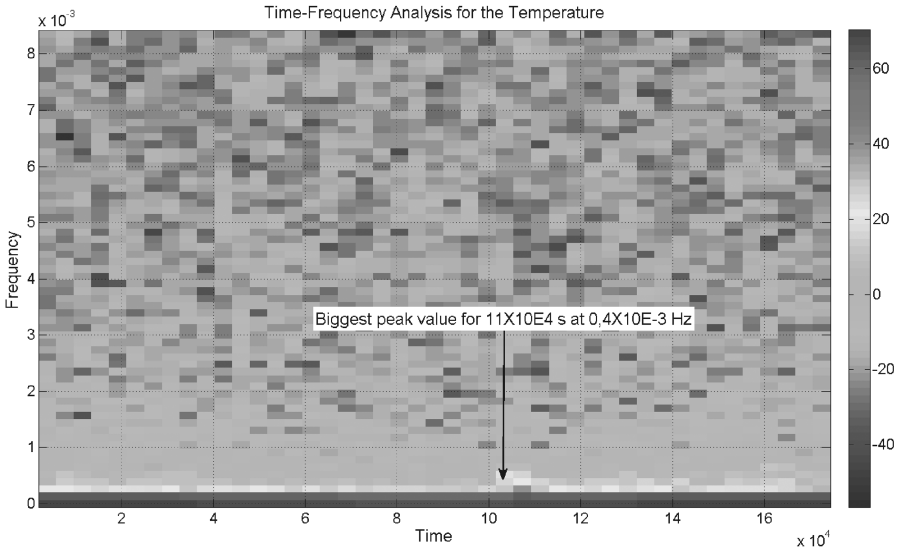

Figure 10. Time-frequency analysis for the temperature.

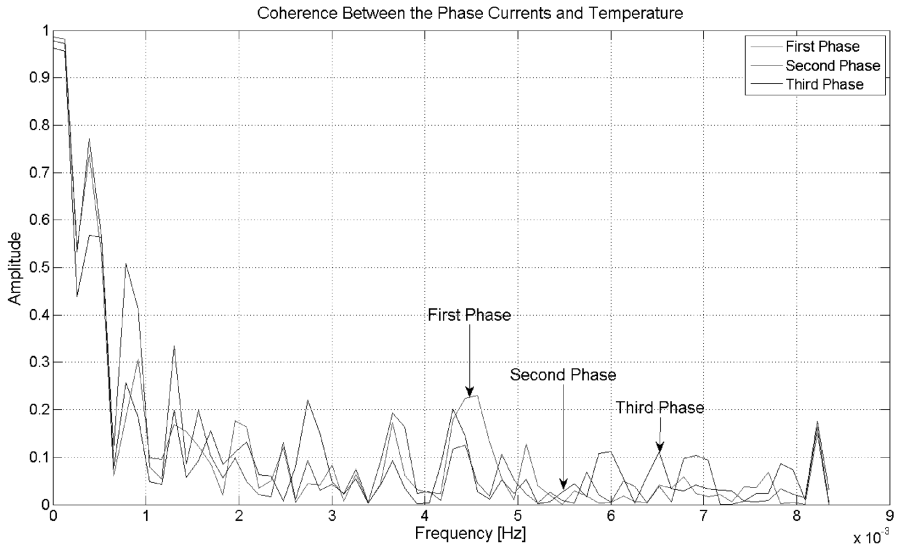

Figure 11. Coherence between the phase currents and temperature.

similarity degree with a correlation level at 0.75 for 0.4×10^{-3} Hz between the first and second phases, the third phase has a low correlation level at around the 0.55 for the same frequency value. This is interpreted as a result of the current imbalances in terms of the third phase; then the low correlation level, which is defined between the third phase and thermal data, shows the distinctions from the other current variations around 0.4×10^{-3} Hz, as seen in Figure 12. Thus, it can be said that this distinction is related to the current imbalances for the third phase.

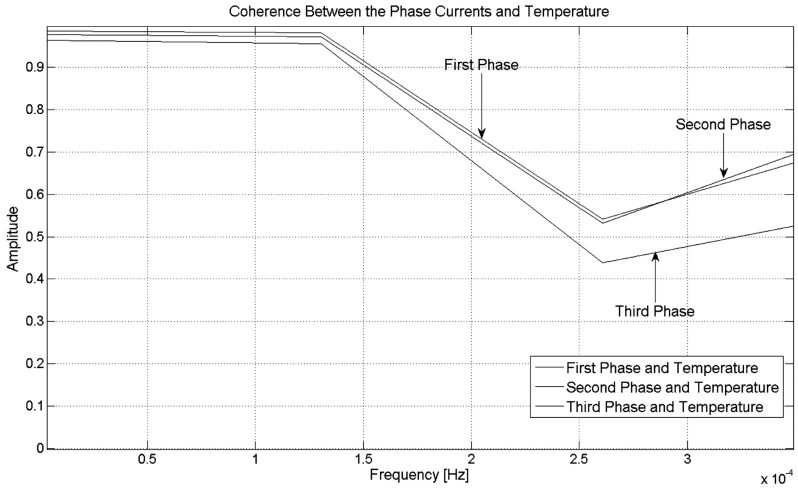

Figure 12. Zoomed coherence variation within narrow frequency band.

5. Conclusions and Discussions

There are two aspects of this research. The first is related to the measurement, and the second is signal analysis. In general, it is the aimed feature extraction approach by signal analysis applications. For this reason, the study purposes the spectral analysis for the current and thermal variations in power cables for a given three-phase system. Under the current imbalances and excessive load conditions, electrical and thermal behaviors of these phases are determined in the frequency domain.

Analyzed data were recorded for a power cable that belongs to a power transformer factory. Current values for each phase of the cables are between 30 A and 250 A, as seen in Figure 4. In addition to this, temperature variation for the cable fluctuates around 30°C–55°C. According to measurement results, all peak values for the first-, second-, and third-phase currents and temperature variation are around 250 A, 245 A, 215 A, and 44°C, respectively.

In terms of the signal analysis, the collected data that contain the phase currents and thermal variation were plotted in the time domain. Hence, the most effective peak value was determined around the 11×10^4 sec in terms of three phase currents, and its frequency value was calculated through the STFT. A huge peak value in the currents was localized in time-frequency domain using the STFT. This localization is given by 11×10^4 sec and 0.4×10^{-3} Hz. After that, the coherence approach, which defines the correlation level among the phase currents and temperature variations in the frequency domain, was used. Considering the low correlation level (around 0.55), the difference of the third phase according to the other phases was emphasized. Hence, this distinction was interpreted as imbalances in current of the third phase. Furthermore, this study presents a new viewpoint in the sense of the signal analysis for electric cable technology.

References

1. Engdahl, G., Edin, H., Eriksson, R., Hörnfeldt, S., and Schönborg, N., "Electrotechnical modeling and design," EEK Annual Report No. A-ETS/EEK-0507, KTH, Stockholm, 2005.
2. Millar, R. J., *Comprehensive Approach to Real Time Power Cable Temperature Prediction and Rating in Thermally Unstable Environments*, Doctoral Dissertation, Helsinki University of Technology, 2006.
3. Zocholl, S. E., and Guzman, A., "Thermal models in power system protection," *Proceedings of the 26th Western Protective Relay Conference*, pp. 1–16, Spokane, WA, 26–28 October 1999.
4. Abou-El-Ela, M. S., Megahed, A. I., and Malik, O. P., "Thermal model based digital relaying algorithm for induction motor protection," *Proc. Canadian Conf. Elect. Comput. Eng.*, Vol. 2, pp. 1016–1019, 1996.
5. Bontempi, G., Vaccaro, A., and Villacci, D., "Power cables thermal protection by interval simulation of imprecise dynamical systems," *IEE Proc. Generat. Transm. Distrib.*, Vol. 151, No. 6, pp. 673–680, 2004.
6. EPRI, "Find hot spots, verify ratings, and increase capacity on underground power cables using distributed fiber optic temperature sensing," field demonstration, 2006.
7. Kovac, N., Sarajcev, I., and Poljak, D., "Nonlinear-coupled electric-thermal modeling of underground cable systems," *IEEE Trans. Power Delivery*, Vol. 21, No. 1, pp. 4–14, 2006.
8. Whitehead, S., and Hutchings, E. E., "Current rating of cables for transmission and distribution," *J. IEE*, Vol. 83, pp. 517–565, 1938.
9. Neher, J. H., and McGrath, M. H., "The calculation of the temperature rise and load capability of cable systems," *Trans. Amer. Inst. Electr. Eng. 111*, Vol. 76, pp. 752–772, 1957.
10. Anders, G. J., *Rating of Electric Power Cables—Ampacity Calculations for Transmission, Distribution and Industrial Applications*, New York: IEEE Press, 1997.

11. Kocar, I., and Ertas, A., "Thermal analysis for determination of current carrying capacity of PE and XLPE insulated power cables using finite element method," *12th IEEE Mediterranean Electrotechnical Conference*, pp. 905–908, Dubrovnik, Croatia, 12–15 May 2004.
12. Anders, G. J., *Rating of Electric Power Cables in Unfavorable Thermal Environment*, New York: IEEE Press Series on Power Engineering, 2005.
13. Walldorf, S. P., Engelhardt, J. S., and Hoppe, F. J., "The use of real-time monitoring and dynamic ratings for power delivery systems and the implications for dielectric materials," *IEEE Elect. Insulat. Mag.*, Vol. 15, No. 5, pp. 28–33, 1999.
14. Vaseghi, S. V., *Advanced Signal Processing and Digital Noise Reduction*, 2nd ed., Great Britian: John Wiley & Sons Ltd. and B. G. Teubner, 2000.
15. Seker, S., and Ayaz, E., "A reliability model for induction motor ball bearing degradation," *Elect. Power Compon. Syst.*, Vol. 31, No. 7, pp. 639–652, 2003.
16. Seker, S., "Determination of air-gap eccentricity in electric motors using coherence analysis," *IEEE Power Eng. Rev.*, Vol. 20, No. 7, pp. 48–50, 2000.
17. Bitter, R., Mohiuddin, T., and Nawrocki, M., *LabVIEW Advanced Programming Techniques*, 1st ed., Boca Raton, FL: CRC Press, 2000.